Investigating Oblique Reconstructions with Super-Resolution in Digital Breast Tomosynthesis

Raymond J. Acciavatti, Stewart B. Mein, and Andrew D.A. Maidment

University of Pennsylvania, Department of Radiology, Physics Section, 1 Silverstein Building, 3400 Spruce St., Philadelphia PA 19104-4206
racci@seas.upenn.edu, Andrew.Maidment@uphs.upenn.edu

Abstract. In digital breast tomosynthesis (DBT), the image of an object is shifted in sub-pixel detector element increments with each increasing projection angle. As a consequence of this property, we have previously demonstrated that DBT is capable of super-resolution in reconstruction planes parallel to the breast support. This study demonstrates that super-resolution is also achievable in obliquely pitched reconstruction planes. To this end, a theoretical framework is developed in which the reconstruction of a sinusoidal input is calculated. It is demonstrated that frequencies exceeding the detector alias frequency can be resolved over many pitches. For experimental validation of this finding, a bar pattern phantom was imaged on a goniometry stand using a commercial DBT system. With a commercial prototype reconstruction solution, high frequency patterns were resolved in oblique reconstructions, and modulation contrast was determined at various pitches and frequencies. This work demonstrates the existence of super-resolution in oblique DBT reconstructions.

Keywords: Digital breast tomosynthesis (DBT), aliasing, super-resolution, image reconstruction, filtered backprojection (FBP), Fourier transform, spectral leakage, oblique reconstruction.

1 Introduction

Digital breast tomosynthesis (DBT) is a 3D imaging modality in which tomographic sections of the breast are generated from a limited range of x-ray projections. Because the image of an object is translated along the detector in sub-pixel detector element increments with each increasing projection angle, our prior work [1] has demonstrated that DBT is capable of super-resolution (*i.e.*, sub-pixel resolution).

By convention, DBT reconstructions are created in planes parallel to the breast support. The feasibility of reconstructions in planes with oblique pitches relative to the breast support has not yet been explored based on the conventional interpretation of the Central Slice Theorem [2]. According to that theorem, Fourier space is sampled only within double-napped cones (DNCs) whose opening angle matches the angular range of the scan. This paper demonstrates that super-resolution is achievable in reconstruction planes whose pitch is well outside the scanning range.

A.D.A. Maidment, P.R. Bakic, and S. Gavenonis (Eds.): IWDM 2012, LNCS 7361, pp. 737–744, 2012.

2 Methods

An analytical framework for investigating super-resolution in obliquely pitched DBT reconstructions is now proposed. Accordingly, we calculate the reconstruction profile along the long axis of a thin input object whose linear attenuation coefficient varies as $C \cdot \cos(2\pi f_0' x')$. In this formulation, f_0' denotes the input spatial frequency, which may be chosen to be higher than the detector alias frequency. In addition, C denotes the amplitude of the input waveform, and x' measures position along the oblique angular pitch ζ relative to point A (Figure 1). The midpoint of the waveform at A is taken to be positioned at the height z_0 above the detector. Under these assumptions, DBT acquisition with a stationary detector and a parallel x-ray beam geometry is modeled for each projection. Although a more general formulation would consider the possibility of a rotating detector and a divergent x-ray beam geometry, the proposed formulation is approximately applicable to measurements made near the midpoint of the chest wall side of a clinical DBT detector.

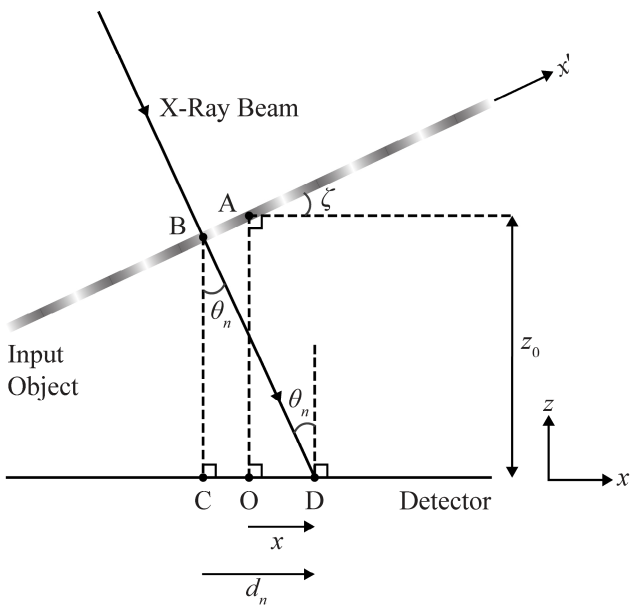

Fig. 1. A schematic diagram of the DBT acquisition geometry is shown (figure not to scale). The thin input object has an attenuation coefficient which varies sinusoidally along the angular pitch ζ. A stationary detector and a parallel beam geometry are modeled for each projection.

As diagrammed in Figure 1, each point along the input object is translated across the detector by the increment d_n in the n^{th} projection. Applying trigonometry to triangle BCD, one can derive an expression for the translational shift d_n as

$$\tan\theta_n = \frac{\overline{\text{CD}}}{\overline{\text{BC}}} = \frac{d_n}{z_0 + (x - d_n)\tan\zeta}\ , \ d_n = \frac{(z_0 + x\tan\zeta)\tan\theta_n}{1 + \tan\zeta\tan\theta_n}\ , \tag{1}$$

where θ_n is the angle of x-ray incidence on the detector for each projection and x is the position along the detector relative to the origin O. In terms of these parameters, the signal recorded by the m^{th} detector element for the n^{th} projection is thus

$$\mathcal{D}\mu(m,n) = \int_{\left[a(m-1/2)-d_{mn}^{-}\right]\sec\zeta}^{\left[a(m+1/2)-d_{mn}^{+}\right]\sec\zeta} C \cdot \cos(2\pi f_0' x)\frac{dx}{a} \quad , \tag{2}$$

where a denotes the length of the detector elements, which are taken to be centered on $x = ma$, and where $d_{mn}^{\pm} \equiv d_n\big|_{x=a(m\pm 1/2)}$. This integral can be evaluated as

$$\mathcal{D}\mu(m,n) = C\sec(\zeta)\mathrm{sinc}(af_0'\sec\zeta)\cos\left(\frac{2\pi f_0'\left[ma - z_0\tan\theta_n\right]\sec\zeta}{1+\tan\zeta\tan\theta_n}\right) , \tag{3}$$

where $\mathrm{sinc}(u) \equiv \sin(\pi u)/(\pi u)$. Using Eq. (3), the reconstructed attenuation coefficient (μ_{FBP}) can now be determined at any point (x, z). The filtered backprojection (FBP) reconstruction is given by the expression

$$\mu_{\text{FBP}} = \frac{1}{N}\sum_m\sum_n \mathcal{D}\mu(m,n)\cdot\left[\phi(t) * \mathrm{rect}\left(\frac{t\sec\theta_n - ma}{a}\right)\right]\Bigg|_{t=x\cos\theta_n + z\sin\theta_n} , \tag{4}$$

where ϕ is the filter and $*$ is the convolution operator [1]. Assuming N projections, the index n ranges from $+(N-1)/2$ to $-(N-1)/2$; the special case $n = 0$ defines the central projection. Following linear systems theory for DBT, the reconstruction filter should be written as the product of a ramp (RA) filter and a spectrum apodization (SA) filter in the Fourier domain, where the SA filter is typically given by a Hanning window function [2]. Both filters are truncated at the frequencies $f = \pm\xi$. The net filter can be calculated in the spatial domain using the inverse Fourier transform [1].

To determine μ_{FBP} along the pitch of the input object, one must evaluate Eq. (4) with the constraints $x = x'\cos\zeta$ and $z = z_0 + x'\sin\zeta$. Finally, to investigate the frequency dependence of the reconstruction, its Fourier transform may also be calculated.

3 Results

3.1 Analytical Modeling

Reconstruction is now simulated for the Selenia Dimensions x-ray unit with 15 projections taken at a uniform angular spacing ($\Delta\theta$) of 1.07°, assuming $C = 1.0$ mm^{-1}, $a = 140$ µm, $f_0' = 0.7a^{-1}$ (5.0 lp/mm), $z_0 = 50.0$ mm, and $\zeta = 20°$. To illustrate the potential for super-resolution, the input frequency has been specified to be higher than the detector alias frequency, $0.5a^{-1}$ (3.6 lp/mm). Also, the pitch of 20° has been chosen since it is well outside the DNCs with an opening angle spanning –7.5° to +7.5° in frequency space.

Figure 2 demonstrates that simple backprojection (SBP) reconstruction is capable of resolving the input frequency, while the central projection alone is not. In acquiring the central projection, the input waveform projects onto the detector as if it were the frequency $f_0' \sec\zeta$ (5.3 lp/mm). Due to aliasing, this frequency is represented as if it were $(1 - 0.7\sec\zeta)a^{-1}$, or 1.8 lp/mm. Consequently, the Fourier transform of the central projection possesses a major peak at 1.8 lp/mm, and has minor alias peaks at $0.7a^{-1}\sec\zeta$ (5.3 lp/mm), $(2 - 0.7\sec\zeta)a^{-1}$ (9.0 lp/mm), and $(1+ 0.7\sec\zeta)a^{-1}$ (12.5 lp/mm). By contrast, the SBP Fourier transform correctly possesses a major peak at the input frequency, 5.0 lp/mm.

FBP reconstructions and their Fourier transforms are also shown using either the RA filter alone or the RA and SA filters together, assuming a filter truncation frequency (ξ) of 10.0 lp/mm. Although ξ is often specified to be the detector alias frequency $0.5a^{-1}$ (3.6 lp/mm), it is necessary to choose a higher value in order to achieve super-resolution. Like SBP, the FBP Fourier transforms possess their major peak at the input frequency, 5.0 lp/mm. Filtering provides an improvement over SBP by smoothing pixilation artifacts in the spatial domain and increasing modulation. The two FBP reconstructions differ in that reconstruction with the RA filter alone has greater modulation than reconstruction with the RA and SA filters together. This finding is expected, since the SA filter places more relative weight on low frequencies to reduce high frequency noise. The drawback of reconstruction with the RA filter alone is increased high frequency spectral leakage in the Fourier domain.

3.2 Experimental Validation

The feasibility of super-resolution in an oblique reconstruction has been verified experimentally using a lead bar pattern phantom. The phantom was placed on a goniometry stand at a height of 7.6 cm above the breast support of a Selenia Dimensions DBT system. The goniometry stand was adjusted to vary the pitch of the bar patterns. At 30 kV and 14 mAs, 15 projections were acquired with a W/Al target-filter combination and a 0.3 mm focal spot. Reconstruction was then performed along the pitch of the bar patterns using a commercial prototype backprojection filtering algorithm (Briona™, Real Time Tomography, Villanova, PA). The pixel size of the reconstruction grid (14.0 μm) was much smaller than that of the detector elements (140 μm), so that the alias frequency of the reconstruction grid (35.7 lp/mm) was significantly higher than the alias frequency of the detector (3.6 lp/mm).

In Figure 3, the central projection is shown at a 0° pitch. As expected, frequencies up to 3 lp/mm can be resolved, since 3 lp/mm is less than the alias frequency of the detector (3.6 lp/mm). Classical signs of aliasing at higher frequencies include Moiré patterns [3] at 4 lp/mm and the misrepresentation of 5 lp/mm as a lower frequency (~3 lp/mm). At the same magnification, the central projection is also shown at a 20° pitch. Its aliasing artifacts are similar to the image at the 0° pitch; the main difference relative to the 0° pitch is compression of the alternating bright and dark bands over a smaller length, increasing the effective frequency projected onto the detector.

Unlike an individual projection, reconstructions along both 0° and 20° pitches clearly show frequencies up to 5 lp/mm (Figure 4). The existence of super-resolution along the 20° pitch is significant because the input frequency is well outside the DNCs in frequency space having an opening angle between –7.5° to +7.5°.

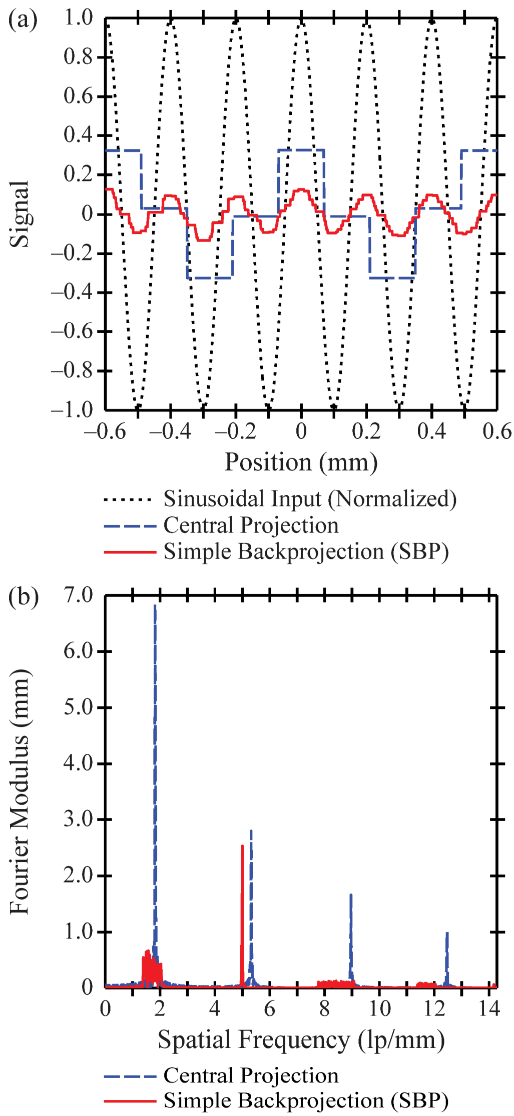

Fig. 2. Assuming $N = 15$, $\Delta\theta = 1.07°$, $C = 1.0$ mm^{-1}, $a = 140$ µm, $f_0' = 5.0$ lp/mm, $\zeta = 20°$, and $z_0 = 50.0$ mm, the central projection and SBP reconstruction are plotted in both the spatial and Fourier domains. The central projection represents the input frequency as 1.8 lp/mm. By contrast, SBP reconstruction performed along the pitch of the input correctly resolves the object. Adding filters to the reconstruction smoothens pixilation artifacts in the spatial domain and increases the modulation relative to SBP. Although the reconstruction with the RA filter alone has the benefit of the highest modulation, it presents the trade-off of increased high frequency spectral leakage. The SA filter suppresses such high frequency Fourier content. The existence of super-resolution along a 20° pitch would not initially be expected from the conventional interpretation of the Central Slice Theorem.

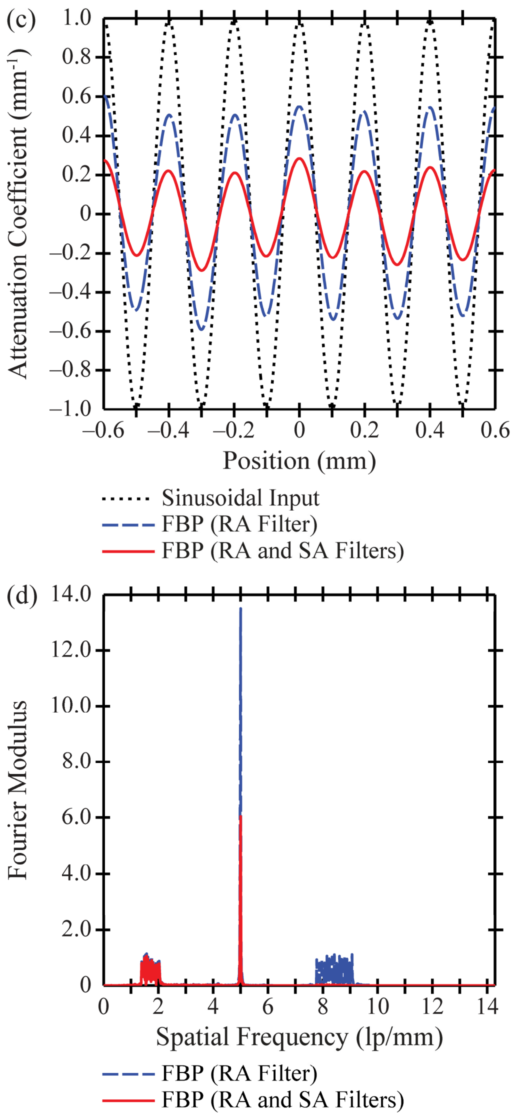

Fig. 2. (*continued*)

Although high frequencies are resolved along a 20° pitch, there is a slight reduction in image quality relative to the 0° pitch. To investigate distortions in visibility, modulation contrast [4] may be calculated as $(I_1 - I_2)/(I_1 + I_2)$, where I_1 and I_2 are the mean signal intensities in the bright and dark bands at a fixed frequency. At 5 lp/mm, modulation contrast is 0.0034 and 0.0020 for 0° and 20° pitches, respectively (41% decrease). The analogous values at 4 lp/mm are 0.0074 and 0.0059 (20% decrease).

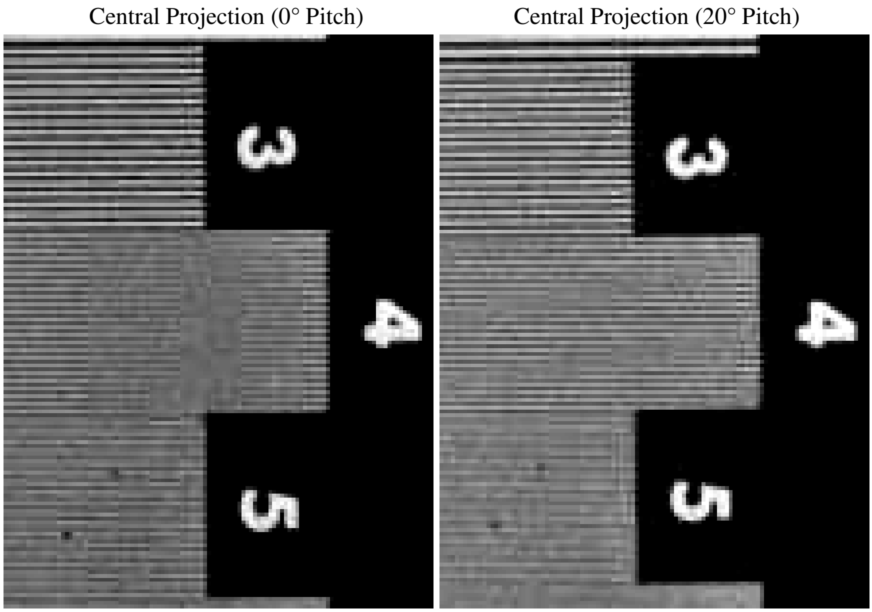

Fig. 3. With a goniometry stand, a lead bar pattern phantom was imaged at various pitches using the Selenia Dimensions DBT system. A single projection can only resolve frequencies less than the alias frequency of the detector, 3.6 lp/mm for 140 μm detector elements. Evidence of aliasing at higher frequencies includes Moiré patterns at 4 lp/mm and the misrepresentation of 5 lp/mm as a lower frequency (~3 lp/mm).

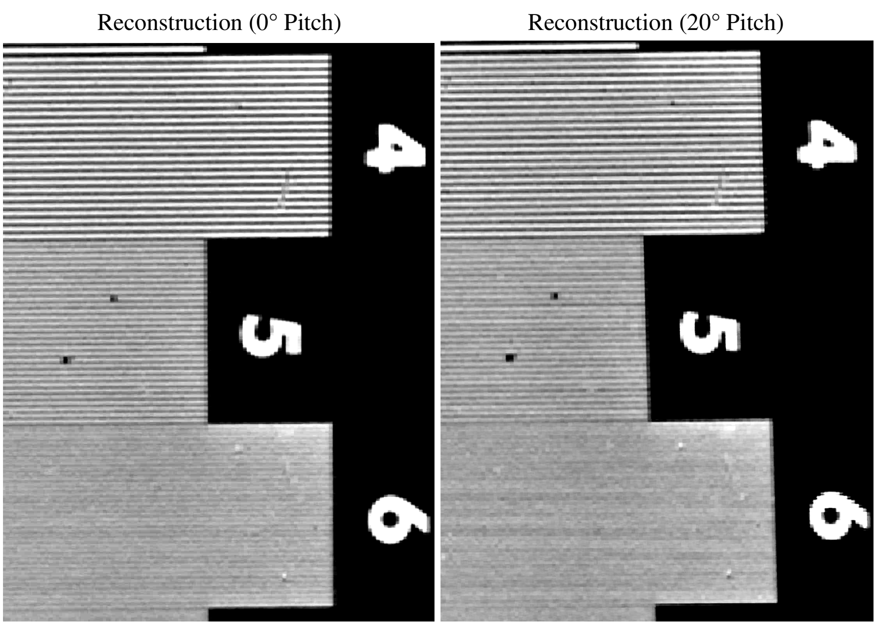

Fig. 4. Reconstructions performed within planes along 0° and 20° pitches can resolve higher frequencies than a single projection (Figure 3), providing experimental evidence of super-resolution.

4 Discussion

This paper demonstrates that high frequency objects can be resolved in obliquely pitched reconstruction planes for DBT. The range of pitches for which super-resolution is feasible is much broader than one would initially expect from the Central Slice Theorem. These analytical predictions were verified experimentally. In future work, the analytical model can be refined by simulating additional subtleties of the imaging system, such as focal spot blur [2] and noise [5, 6]. Also, filters with more parameters can be modeled, and the parameters can be optimized for different pitches.

Acknowledgments. We thank Roshan Karunamuni (UPenn) for his help assembling the goniometry stand, as well as Johnny Kuo, Susan Ng, and Peter Ringer (Real Time Tomography) for their assistance reconstructing the bar pattern images. The project described was supported by predoctoral training Grant No. W81XWH-11-1-0100 through the Department of Defense Breast Cancer Research Program. The content is solely the responsibility of the authors and does not necessarily represent the official views of the funding agency. Andrew D. A. Maidment is the chair of the Scientific Advisory Board of Real Time Tomography.

References

1. Acciavatti, R.J., Maidment, A.D.A.: Investigating the potential for super-resolution in digital breast tomosynthesis. In: Pelc, N.J., Samei, E., Nishikawa, R.M. (eds.) Proc. of SPIE, Medical Imaging 2011: Physics of Medical Imaging, vol. 7961, pp. 79615K-1–79615K-12. SPIE, Bellingham (2011)
2. Zhao, B., Zhao, W.: Three-dimensional linear system analysis for breast tomosynthesis. Med. Phys. 35(12), 5219–5232 (2008)
3. Albert, M., Beideck, D.J., Bakic, P.R., Maidment, A.D.A.: Aliasing effects in digital images of line-pair phantoms. Med. Phys. 29(8), 1716–1718 (2002)
4. Barrett, H.H., Swindell, W.: Radiological Imaging: The Theory of Image Formation, Detection, and Processing, New York (1981)
5. Barrett, H.H., Myers, K.J.: Foundations of Image Science. Bahaa E.A. Saleh, Hoboken (2004)
6. Hu, Y.-H., Masiar, M., Zhao, W.: Breast Structural Noise in Digital Breast Tomosynthesis and Its Dependence on Reconstruction Methods. In: Martí, J., Oliver, A., Freixenet, J., Martí, R. (eds.) IWDM 2010. LNCS, vol. 6136, pp. 598–605. Springer, Heidelberg (2010)